SYNCHROTRON SIDEBANDS IN BETATRON OSCILLATION MEASURED BY MEANS OF RF KNOCKOUT IN THE PF STORAGE RING

T. Katsura, Y. Kamiya and S. Shibata
National Laboratory for High Energy Physics
Oho-machi, Tsukuba-gun, Ibaraki-ken, 305, Japan

ABSTRACT

Both incoherent and coherent synchrotron sidebands were observed in the betatron oscillation by using the RF knockout system. The oscillation was detected by receiving the synchrotron light from the beam to a position sensing photodiode. The oscillation signal is analyzed with a spectrum analyzer. Results are compared with a theoretical model.

INTRODUCTION

The betatron sidebands in the PF storage ring were observed by use of the RF knockout (RFKO) system, which had earlier been introduced for the measurement of tune parameters. By exciting the beam with transverse magnetic field, we observed transverse beam oscillations with a position-sensing photodiode array which detected the synchrotron light from the beam. The photodiode signal was fed to a spectrum analyzer to obtain the frequency distribution. Both incoherent and coherent longitudinal oscillations were distinguished in the distribution and their amplitudes were compared with theoretical predictions. Also their chromaticity dependence was obtained to test the theoretical model.

THEORETICAL MODEL

Theoretical foundation on the subject is given in a paper by D.E.P. Mohl and P.L. Morton[1]. They indicate that it should be possible experimentally to obtain both incoherent and coherent longitudinal oscillation frequencies by measuring the coherent transverse oscillation response.

Equation of Motion

An off-momentum particle with momentum $p = p_o + \Delta p$ will have a shift in the betatron frequency ω_β given by

$$\Delta\omega_\beta = \xi\left(\frac{\Delta p}{p}\right)\omega_r \qquad (1)$$

with $\xi = (p/\omega_r)(\partial\omega_\beta/\partial p)$ and revolution frequency ω_r as well as a longitudinal phase oscillation of frequency $\omega_s = 2\pi f_s$.

The equation of transverse motion for the ℓ-th particle is described as

$$\ddot{x}_\ell + (\omega_{\beta o} + \Delta\omega_{\beta\ell})^2 x_\ell = F\cos\omega_d t \qquad (2)$$

The right hand side is the driving force from the RFKO at frequency ω_d.

The longitudinal motion of the ℓ-th particle is given by

$$\Delta p_\ell/p = A_\ell\cos(\omega_{si}t + \alpha_\ell) + B\cos(\omega_{sc}t + \beta) \qquad (3)$$

where A_ℓ, ω_{si} and α_ℓ are the amplitude, frequency, and phase of the incoherent longitudinal motion of the ℓ-th particle and where B, ω_{sc} and β are of the coherent motion in common for all the particles. Using (1) and (3), the solution of Eq. (2) is approximately given by

$$x_\ell(n) = \frac{FJ_n(\Delta\omega/\omega_s)}{2\omega_{\beta o}(\omega_{\beta o} + n\omega_s - \omega_d)} \times \sum_{m=-\infty}^{+\infty} J_m\left(\frac{\Delta\omega}{\omega_s}\right)\cos\left[\omega_d t - (n-m)(\omega t + \alpha)\right] \qquad (4)$$

where expression $\Delta\omega_{\beta\ell} = \Delta\omega\cos(\omega_s t + \alpha)$ is used.

Incoherent Longitudinal Oscillation

If only the incoherent phase motion presides, Eq. (4) is described with $\alpha = \alpha_\ell$ and the ensemble average of x_ℓ is expressed with a term only for m = n, since α_ℓ is randomly distributed. The sideband resonances can be seen at the driving frequency $\omega_d = \omega_{\beta o} + n\omega_{si}$ and are spaced by ω_{si}. The ratio of the n-th amplitude to the fundamental peak (n = 0) is given by

$$\frac{|\langle x(n)\rangle|}{|\langle x(o)\rangle|} = \frac{\langle J_n^2(\xi A/\nu_{si})\rangle}{\langle J_o^2(\xi A/\nu_{si})\rangle}$$

with $\nu_{si} = \omega_{si}/\omega_r$.

Assuming the $\Delta p/p$ distribution to be Gaussian and setting $x = \xi\sigma_\varepsilon/E\,\nu_{si}$ with $\sigma_\varepsilon/E = (\Delta p/p)$ r.m.s., the ratio is given

$$\frac{|\langle x(n)\rangle|}{|\langle x(o)\rangle|} = \frac{I_n(x^2)}{I(x^2)} \to \frac{1}{2^n n!}\left(\frac{\xi}{\nu_{si}}\,\frac{\sigma_\varepsilon}{E}\right)^{2n} \qquad (5)$$

and approximated for $x \ll 1$.

Coherent Longitudinal Oscillation

If only the coherent phase motion exists, Eq. (4) is interpreted with $\alpha = \beta$ and $\Delta\omega/\omega_s = \xi B/\nu_{sc}$ in common for every particle and all the sidebands can be excited by driving any one of the resonances. For the driving freuqnecy $\omega_d = \omega_{\beta o} + n\omega_{sc}$, the spectrum includes two components:

$$|\langle x(n)\rangle|_n \propto \langle J_n^2(\xi B/\nu_{sc})\rangle \text{ at } \omega_d$$

and

$$|\langle x(n)\rangle|_o \propto \langle J_o(\xi B/\nu_{sc})J_n(\xi B/\nu_{sc})\rangle \text{ at } \omega_{\beta o}.$$

Usually $\xi B \ll \nu_{sc}$. The fundamental mode will hence dominate

$$\frac{|\langle x(n)\rangle|_n}{|\langle x(n)\rangle|_o} \simeq \frac{1}{n!}\left(\frac{\xi B}{2\nu_{sc}}\right)^n \qquad (6)\ .$$

EXPERIMENTAL SETUP

Figure 1 shows a block diagram of the experimental setup. The system has already been used for measuring tune parameters during operation periods[2]. Only a brief description is given below. The observation system consists of two parts, one to excite the beam and the other to detect its oscillations.

If the excitation frequency is, for example, set at $f_r * \Delta Q$ where f_r is the revolution frequency and ΔQ is the fractional part of the betatron wave number Q, the detection system gives a peak at the chosen frequency.

RF Knockout System

A RFKO system is used to excite the beam. Four rods placed parallel to the beam are driven with their individual current sources to make a magnetic field transverse to the beam. The phase relation among the rods decides the direction of the field in either horizontal or vertical. The signal generator produces continuous sinusoidal signal at a fixed frequency with an amplitude suitably adjusted for the excitation of the beam. Care must be taken not to give excessive driving power and force the beam to oscillate at any given frequency, which is named here "through".

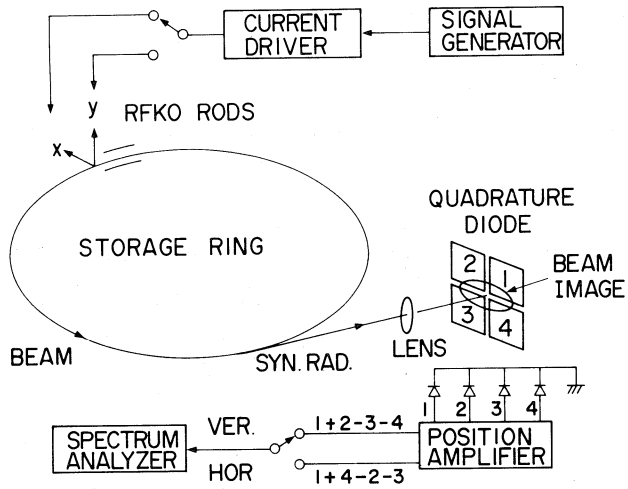

Fig. 1 Experimental setup: RF knockout system with its signal generator at the top and the analyzing system with a position-sensing photodiode at the bottom.

Oscillation Detecting System

To detect the oscillation of the beam, the synchrotron light from the beam was led to a photodiode on which the beam image is focused with optical lenses. The photodiode detector is an array made up of four quadrants. Four outputs from the diode are orderly added and subtracted in an analog amplifier to separate both horizontal or vertical signals of the oscillating beam.

Either of the two signals is chosen corresponding to the direction of excitation field and fed to the spectrum analyzer.

Calibration of System

As we have to compare the strengths of sidebands, we calibrated both RFKO and detection systems over the range of frequencies necessary for the measurement. The RFKO system has irregular response for such a wide frequency range. The frequency response of the RFKO system is taken into account in the data processing.

The detector system, on the contrary, shows much simpler frequency response which varies only monotonically within 10% over the frequency range concerned.

MEASUREMENTS AND RESULTS

Three kinds of measurements were made. First, the beam was excited at betatron frequencies f_x, f_y and their sidebands stepped by $\pm nf_s$. Second, their chromaticity dependence was observed at $f_{x,y} \pm f_s$ by changing the current of the defocusing sextupole magnets. Third, there are such cases that the main peak is enhanced more strongly than the sideband at a new driving frequency differing only by a few kHz from that used in the first measurement made above. This is the case when the longitudinal phase oscillation is coherent.

Betatron Sidebands Due to Incoherent Longitudinal Oscillation

Figure 2 shows a typical picture of the spectrum taken with the spectrum analyzer. The excitation frequency was set at the horizontal betatron frequency f_x. Four sharp peaks are seen sticking above two other smooth hilly peaks wide as 200 kHz or more, which is background of the photodetector system including the amplifier. The peak at the lefthand side is the "zero" for the scanning. The second sharp peak is the main peak at f_x and the third one is also the main peak at $f_r - f_x$. The right most peak gives merely f_r. The excitation frequency was changed by step of f_s and sideband peaks are searched near at each step. To

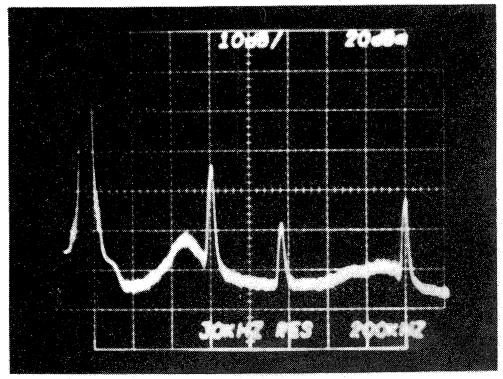

Fig. 2 Typical spectrum taken with the driving frequency at 626 kHz and the generator power level at 100 dB. The scope settings are Hor. 200 kHz/div. and Ver. 10 dB.div.

obtain a peak above the background, the excitation power level often had to be adjusted depending on where the peak is; when it is in the hill region of the background, the driver power level must be raised compared to other region. Due to this background, we often observed the beam being forced to oscillate at any frequency. When this much power level was required, we also took data called "through" by shifting the driving frequency aside so as to later subtract the "through" signal from the measured signal at the aimed sideband.

The peaks obtained above with different driver power levels are normalized to one specific value of power level and corrected for the frequency response of the RFKO and photodiode system.

The data are taken for different current values with both uniform and partial fillings of RF buckets[2]. Figure 3 shows a spectrum for sidebands obtained with beam partially filled and its current of 120 mA. For f_x, peaks are seen clearly at $\pm f_s$ and $+2f_s$ but the peak at $-2f_s$ seems to be hidden in the background hill. For f_y, sidebands up to $\pm 2f_s$ are clearly seen. But they barely stick out of the background at $\pm 3f_s$. Only their upper limits are shown with arrows.

Theoretical values of spectrum strengths are also shown in dB with respect to the main peak with the mode number attached.

In this high current data, the first sidebands are especially broadened in both horizontal and vertical directions, which is indicated with triangular peaks in

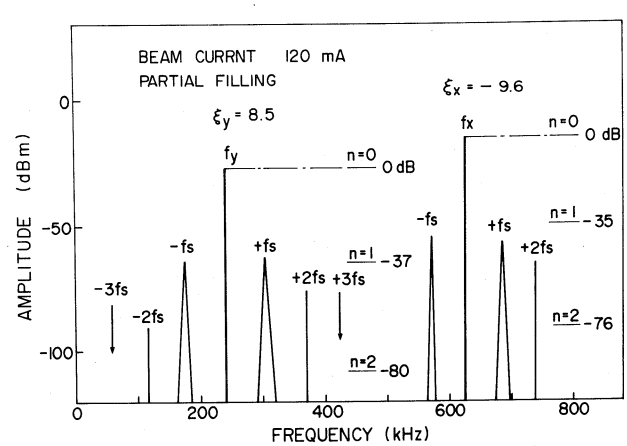

Fig. 3 Synchrotron sidebands of f_x and f_y taken with beam current of 120 mA. Theoretical values are shown with horizontal broken lines for mode n. Broad peaks are shown in triangular shape to indicate their widths.

the figure. No broadening was, however, observed in low current data. This fact hints there may be ion-trapping[3]. But, it would also be possible to attribute it to so called "758" instability pertinent to the RF system. Further study will be needed to determine which is causing the broadening. An independent observation of ion-trapping is discussed in another paper submitted to this symposium[3].

Chromaticity Dependence

To test the theoretical model, the strength of first sidebands were measured for different values of chromaticity. Figure 4 shows the amplitudes of first vertical sidebands $f_y \pm f_s$ when the chromaticity ξ_y was changed. Theoretical values from Eq. (5) are shown with solid lines. The amplitude of $f_y \pm f_s$ are normalized to the amplitude of the main peak.

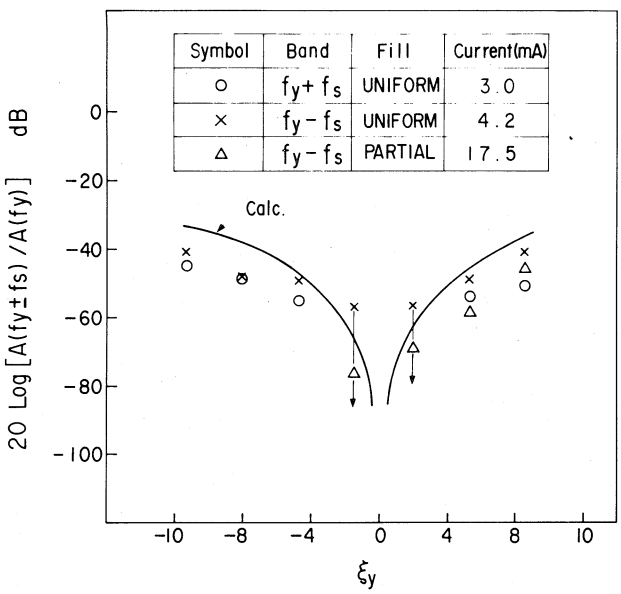

Fig. 4 Chromaticity dependence of sidebands $f_y \pm f_s$ taken with uniform or partial beam filling. Theoretical values are shown with solid curves. Amplitudes are shown by assigning them to $A(f_y) = |\langle x(0)\rangle|$ and $A(f_y \pm f_s) = |\langle x(1)\rangle|$ in Eq. (5).

Betatron Sidebands Due to Coherent Longitudinal Oscillation

According to the theoretical consideration, it is predicted there exists sideband frequencies which enchance the main peak higher than the sidebands at the driving frequency. Searching carefully near the sidebands, we found that the main peak pronounced higher than the sidebands at frequencies differing by a few kHz from that of the incoherent case. Table 1 summarizes these cases. Mode number n in Column 1 indicates the driving frequency is set at $f_d = f_\beta + nf_s$. Two kinds of spectrum amplitudes are taken at frequencies $f = f_\beta$ and $f_\beta \pm nf_s$ and given as R(f) in Column 2 and 3. All the amplitudes (in dB) are normalized to the amplitude of the main peak taken with the driving frequency at $f_d = f_\beta$.

Data are also taken with RF phase modulation turned on. The RF phase was modulated with a 56 kHz cw source[5]. Figure 5 shows the spectrum with the main peak as well as sidebands at $f_y \pm f_s$. Results are listed in the table with symbol * to compare with data without the phase modulation.

By defining a as the amplitude normalized to σ_ξ/E, theoretical predictions from Eq. (6) are also added to the table. They lie near to the experimental results

Table 1

Coherent sideband amplitudes measured at f_y and $f_y \pm nf_s$ when the driving frequency was set at $f_d = f_y \pm nf_s$ for n = 1, 2 and the chromaticity $\xi_y = 8.5$. The definition of R(f) is given in the text. Theoretical calculation is given for the amplitude a = 1.5 ∿ 0.2. Symbol * indicates that the data was taken with RF phase modulation on.

MODE NO.		R(fy) dB	R(fy ± nfs) dB
n = 1	Calc.	−18 ∼ −38	−36 ∼ −76
	Expt.*	−23	−37
	Expt.	−44	−51
n = 2	Calc.	−42 ∼ −77	−84 ∼ −154
	Expt.	−33	−57

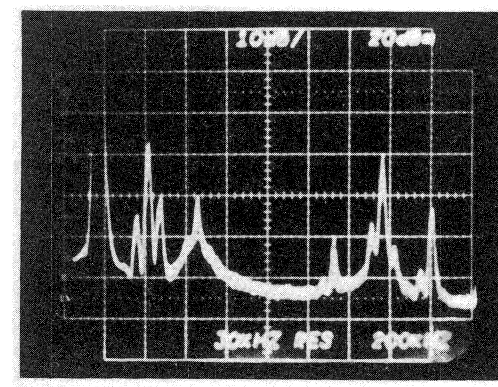

Fig. 5 Spectrum with the driving frequency at 293.8 kHz ($f_y + f_s$) while RF phase modulation is applied.

within the parameter a = 1.5 - 0.2. Data with n = 2 exhibit some tendency similar to those with n = 1 but do not agree with the prediction to the same extent.

ACKNOWLEDGEMENTS

We are indebted to greatly thank Prof. K. Huke, head of the light source division for his useful discussion. We also express our gratitude to the crew for operating the storage ring and their invaluable cooperation.

REFERENCES

1. D.E.P. Mohl and P.L. Morton, PEP-68, 1973 PEP Summer Study (1974).
2. PHOTON FACTORY ACTIVITY REPORT, p.IV-27 and p.IV-42 (1982/83).
3. M.E. Biagini et al., Observation of ion-trapping at ADONE, 11th International Conference on High Energy Accelerators, CERN, p.687 (1980).
4. Y. Kamiya et al, Vertical instability caused by ion-trapping in KEK-PF, contributed to this symposium.
5. H. Kobayakawa, Y. Yamazaki and Y. Kamiya, KEK-83-8 (1983).